Intense upconversion and infrared emissions in Er³⁺–Yb³⁺ codoped Lu₂SiO₅ and (Lu₀.₅Gd₀.₅)₂SiO₅ crystals

Lin Han,[1] Feng Song,[1,a)] Shu-Qi Chen,[1] Chang-Guang Zou,[1] Xiao-Chen Yu,[1]
Jian-Guo Tian,[1] Jun Xu,[2] Xiao-dong Xu,[2] and Guang-jun Zhao[2]

[1]*Photonics Center, College of Physics, Nankai University, Tianjin 300071, People's Republic of China*
[2]*Shanghai Institute of Optics and Fine Mechanics, Chinese Academy of Sciences, Shanghai 201800,
People's Republic of China*

High optical quality Lu₂SiO₅ (LSO) and (Lu₀.₅Gd₀.₅)₂SiO₅ (LGSO) laser crystals codoped with Er³⁺ and Yb³⁺ have been fabricated by the Czochralski method. Intense upconversion (UC) and infrared emission (1543 nm) are observed under excitation of 975 nm. The luminescence processes are explained and the emission efficiencies are quantitatively obtained by measuring the UC efficiency and calculating the emission cross section. The temperature-dependent optical properties of the crystals are also investigated. Our study indicates that Er³⁺–Yb³⁺:LSO and Er³⁺–Yb³⁺:LGSO crystals are promising gain media for developing the solid-state 1.5 μm optical amplifiers and tunable UC lasers. © 2008 American Institute of Physics. [DOI: 10.1063/1.2954010]

Er³⁺ doped materials have been attracting intensive research attention for their excellent performance in upconversion (UC) and near infrared (NIR, near 1.5 μm) emission.[1–3] It is well known that different host materials significantly affect the emission performance of the rare-earth ions, thus considerable research effort has been spent on investigating efficient hosts. Silicate crystals have been actively investigated recently as the photoluminescence material because of their low symmetry, high quantum efficiency, and superior luminescence properties. Remarkable luminescence and laser performance have been achieved in Yb³⁺ doped Gd₂SiO₅ (GSO), Lu₂SiO₅ (LSO), Y₂SiO₅ (YSO), and Er³⁺–Yb³⁺ codoped GSO crystals.[4–6]

In this letter, we present the fabrication, luminescence and thermal properties of Er³⁺–Yb³⁺ codoped LSO and (Lu₀.₅Gd₀.₅)₂SiO₅ (LGSO) crystals. LSO and LGSO crystals have been studied exclusively as the scintillator materials doped with Ce³⁺ and they have not yet been investigated as the luminescence or laser material when codoped with Er³⁺ and Yb³⁺. Our study shows that Er³⁺–Yb³⁺:LSO and Er³⁺–Yb³⁺:LGSO crystals present not only intense visible UC but also good NIR emission under 975 nm excitation. Their UC efficiencies can be compared to those of fluoride glass. Meanwhile, highly efficient NIR emission at 1543 nm are also obtained over a wide temperature range.

LSO and LGSO single crystals codoped with Er³⁺ and Yb³⁺ have been grown by the Czochralski method. The parameters are listed in Table I. The luminescence spectra were obtained using a fluorescence spectrophotometer (model F111AI) under the 975 nm laser diode (LD) excitation. The UC emission efficiencies were measured by bandpass filter and power meter. The temperature of the crystal is controlled from 260 to 470 K through a copper sample mount, which can be heated by a resistance wire element and cooled by a thermoelectric cooler. A copper-constantan thermocouple is attached to one facet of the crystal sample to monitor the temperature within an accuracy of 0.5 °C.

TABLE I. Physical parameters of Er³⁺–Yb³⁺:LSO and Er³⁺–Yb³⁺:LGSO.

Sample	Concentration ($\times 10^{20}/cm^3$)		Thickness (mm)	Density (g/cm^3)
	Er³⁺	Yb³⁺		
LSO	0.868	28.9	0.74	7.4
LGSO	0.867	28.9	0.76	7.1
	Refractive Index		Space Group	E_{phonon}
LSO	1.82		C2/c	970 cm⁻¹
LGSO	1.80		C2/c	1194 cm⁻¹

Figure 1 shows the UC emission spectra of Er³⁺–Yb³⁺:LSO and Er³⁺–Yb³⁺:LGSO at 300 K when the pump power of the 975 nm LD is fixed at 278 mW. Green and red emission bands of these two crystals are clearly observed, and their emission bands are very broad with multiple peaks. The UC efficiencies were measured and the normalized UC efficiency η_{up} are listed in Table II. The values in LSO and LGSO crystals are higher than those in tellurite, phosphate, and silicate glasses, and comparable to those in
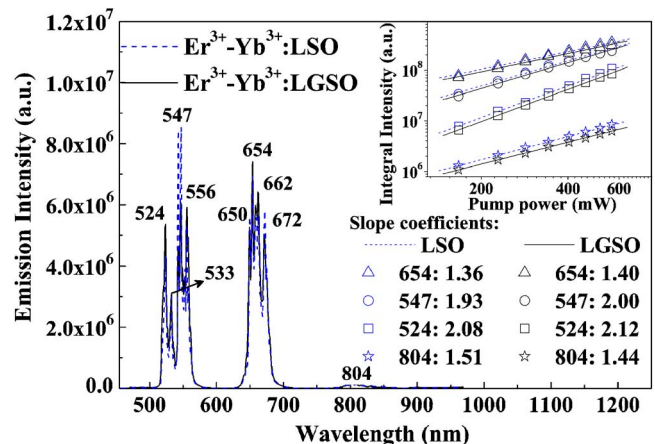
FIG. 1. (Color online) UC spectra of Er³⁺–Yb³⁺:LSO and Er³⁺–Yb³⁺:LGSO at 300 K under 975 nm LD excitation. Inset is log-log plots of the integrated emission intensities vs the excitation power.

a)Author to whom correspondence should be addressed. Tel.: +86-22-2350-3620. FAX: +86-22-2350-6238. Electronic mail: fsong@nankai.edu.cn.

TABLE II. Standardized UC efficiency (η_{up}) in different Er^{3+}–Yb^3 codoped materials.

	LSO[a]		LGSO[a]		Bismuth[b]		Tellurite[c]	Fluoride[d]	Silicate[d]	Phosphate[d]
	Green	Red	Green	Red	Green	Red	Green	Green	Green	Green
η_{up}	0.89×10^{-3}	1.04×10^{-3}	0.83×10^{-3}	0.93×10^{-3}	1.3×10^{-3}	3.13×10^{-4}	0.95×10^{-4}	1×10^{-3}	2×10^{-7}	6×10^{-8}

[a]Our work.
[b]Reference 7
[c]Reference 8.
[d]Reference 9.

bismuth and fluoride glasses. In addition, the UC efficiencies of Er^{3+}–Yb^{3+}:LSO are higher than those of Er^{3+}–Yb^{3+}:LGSO. This is because the phonon energy of LSO is lower than that of LGSO, which reduces the possibilities of some nonradiative processes and enhances the UC efficiencies.

The inset in Fig. 1 plots the integrated emission intensities versus the excitation power using the log-log scale. The slope efficiencies of the Er^{3+}–Yb^{3+}:LSO/Er^{3+}–Yb^{3+}:LGSO with respect to the emission bands of 524, 547, 654, and 804 nm are 2.08/2.12, 1.93/2.00, 1.36/1.40, and 1.51/1.44, respectively. From these data, we can thus conclude that Er^{3+}–Yb^{3+}:LSO and Er^{3+}–Yb^{3+}:LGSO have the same populating mechanism: the $^2H_{11/2}$, $^4S_{3/2}$, $^4F_{9/2}$, and $^4I_{9/2}$ levels of Er^{3+} are populated by two-photon processes; while the populating mechanisms of $^4F_{9/2}$ and $^4I_{9/2}$ levels must contain some one-photon processes. As been shown in Fig. 2, initially, Yb^{3+} ions transfer the absorbed 975 nm photon energy to Er^{3+} via energy transfer (ET) processes [(a)–(c) in Fig. 2], and thus populate the $^4I_{9/2}$, $^4F_{9/2}$, and $^4F_{7/2}$ levels of Er^{3+}. After two-photon absorption processes, the $^4I_{13/2}$, $^4I_{9/2}$, $^2H_{11/2}$, and $^4S_{3/2}$ levels are subsequently populated by multiphonon assistant relaxations (MPR) (W_{ij}^{NR} in Fig. 2). Finally, Er^{3+} ions return to the ground state from these levels through radiative emissions. Furthermore, after the $^4I_{13/2}$ and $^4I_{11/2}$ levels are populated by the one-photon process, some ion-ion interactions [(d)–(f) in Fig. 2] also help to populate $^4F_{9/2}$ and $^4I_{9/2}$ levels. Therefore, $^4F_{9/2}$ and $^4I_{9/2}$ levels are populated by a combined one-photon and two-photon processes.

Figure 3 is the NIR emission spectra of Er^{3+}–Yb^{3+}:LSO and Er^{3+}–Yb^{3+}:LGSO at 300 K when the pump power of the 975 nm LD is fixed at 278 mW. The emission centered at 1543 nm is due to the $^4I_{13/2} \rightarrow {}^4I_{15/2}$ transition of Er^{3+}. The full width of half maximum of the 1543 nm emission is 38 nm for Er^{3+}–Yb^{3+}:LSO and 42 nm for Er^{3+}–Yb^{3+}:LGSO. Emission cross sections (σ_{em}) are calculated from the emission spectra with the Füchtbauer–Ladenburg (FL) formula[13]

$$\sigma_{em}(\lambda) = \frac{\lambda^5 I(\lambda)}{8\pi n^2 c \tau \int \lambda I(\lambda) d\lambda}. \tag{1}$$

Here, $I(\lambda)$ is the emission intensity, c is the velocity of light in the vacuum, n is the refractive index, and τ is the lifetime of the $^4I_{13/2}$ energy level of Er^{3+}, and can be derived from the fluorescence decay measurements (5.15 ms for Er^{3+}–Yb^{3+}:LSO and 4.43 ms for Er^{3+}–Yb^{3+}:LGSO). The inset of Figure 3 shows the calculated cross sections and the values are listed in Table III. The values in the silicate crystals (YSO, GSO, LSO, and LGSO) are comparable to those in tellurite and phosphate glasses that have been demonstrated with high efficient laser emission at 1.5 μm. The 1.5 μm emission cross section of Er^{3+}–Yb^{3+}:LGSO is larger than that of Er^{3+}–Yb^{3+}:LSO because the larger phonon energy of LGSO enhances the population at $^4I_{13/2}$ level by MPR processes.

Temperature dependence of the UC and NIR emission intensities have been investigated from 260 to 470 K. Applying the models developed for other Er^{3+}–Yb^{3+} codoped systems,[14] the temperature dependence can be explained by conventional rate equations using the ET mechanisms described in Fig. 2. Figure 4 shows the temperature evolution of the experimental intensities and theoretical fitting results.

In the visible emissions, the intensities of 547 and 654 nm decrease as the temperature increases. This effect

FIG. 2. (Color online) Energy levels and ET processes of Er^{3+}–Yb^{3+}:LSO and Er^{3+}–Yb^{3+}:LGSO. [(a)–(c)] ET, W_{ij}^{NR}: MPR, (d) cooperative UC, and [(e) and (f)] cross relaxation.

FIG. 3. (Color online) NIR emission spectra of Er^{3+}–Yb^{3+}:LSO and Er^{3+}–Yb^{3+}:LGSO at 300 K under 975 nm LD excitation. The inset is the emission cross section calculated by the FL formula.

TABLE III. Emission cross sections (σ_{em}) of Er^{3+} ($^4I_{13/2} \rightarrow {}^4I_{15/2}$) in different host materials.

	LSO[a]	LGSO[a]	YSO[b]	GSO[b]	YCOB[b]	YAG[b]	Tellurite[c]	Phosphate[d]	AYF[e]
σ_{em} ($\times 10^{-20}$ cm^2)	0.793	0.994	0.8	1.03	0.6	1.5	0.852	0.78	0.549

[a]Our work.
[b]Reference 10.
[c]Reference 8.
[d]Reference 11.
[e]Reference 12.

can be explained from two aspects. First, as the temperature increases, nonradiative MPR rates are enhanced to weaken the radiative transitions at the same level. Secondly, the improved MPR processes also shorten the lifetimes of some of the middle energy levels involved in the UC process ($^4I_{11/2}$ and $^4I_{13/2}$), thus reduce the possibility of the photon absorption that follows. As for the 524 nm signal, the major reason for the intensity to increase slightly as the temperature grows should be attributed to the enhanced population at $^2H_{11/2}$ level via MPR process. It is to be noted that because the thermal distribution of the population between $^4S_{3/2}$ and $^2H_{11/2}$ is very sensitive to temperature, the emission intensity of 524 nm is not very stable, especially for LSO.

In the NIR emission, the consistent increasing of the intensity near 1543 nm as the temperature grows can be explained as the following. First of all, the main depopulating mechanism of $^4I_{13/2}$ level is the ion-ion interactions [(d)–(f) in Fig. 2] because the MPR process from $^4I_{13/2}$ to the ground level can be neglected due to its large energy separation. Thus, the depopulation rate of $^4I_{13/2}$ level only depends on the ion concentration. At the same time, the MPR processes from the upper levels populating the $^4I_{13/2}$ level are enhanced as the temperature increases, resulting in an improved emis-

sion rate from the $^4I_{13/2}$ level to the ground state.

To summarize, strong UC and NIR emissions are demonstrated in Er^{3+}–Yb^{3+}:LSO and Er^{3+}–Yb^{3+}:LGSO crystals under 975 nm excitation. Their normalized UC efficiencies can reach up to 0.89×10^{-3} (LSO, green), 1.04×10^{-3} (LSO, red), 0.83×10^{-3} (LGSO, green), and 0.93×10^{-3} (LGSO, red). Meanwhile, highly efficient NIR emission at 1543 nm ($\sigma_{emLSO} \geq 0.793 \times 10^{-20}$ cm^2, $\sigma_{emLGSO} \geq 0.994 \times 10^{-20}$ cm^2) are also obtained over a wide temperature range (300–470 K). These results indicate that Er^{3+}–Yb^{3+}:LSO and Er^{3+}–Yb^{3+}:LGSO crystals are good candidates as the gain medium for solid-state optical amplifiers at 1.5 μm as well as tunable UC lasers.
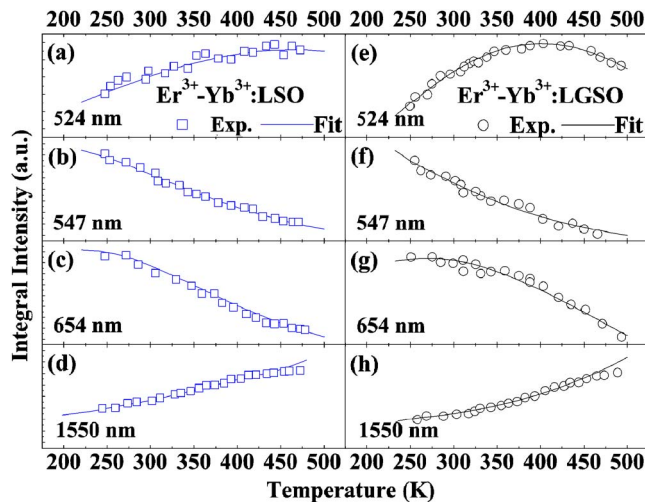
FIG. 4. (Color online) Temperature evolution of the experimental intensities and theoretical fitting results. The pump power of 975 nm LD is fixed at 278 mW. [(a)–(d)] Er^{3+}–Yb^{3+}:LSO, and [(e)–(h)] Er^{3+}–Yb^{3+}:LGSO.

[1]S. Gallis, M. Huang, and A. E. Kaloyeros, Appl. Phys. Lett. **90**, 161914 (2007).
[2]D. M. da Silva, L. R. P. Kassab, S. R. Lüthi, C. B. de Araújo, A. S. L. Gomes, and M. J. V. Bell, Appl. Phys. Lett. **90**, 081913 (2007).
[3]F. Song, K. Zhang, J. Su, L. Han, J. Liang, X. Z. Zhang, L. H. Yan, J. G. Tian, and J. J. Xu, Opt. Express **14**, 12584 (2006).
[4]W. X. Li, Q. Hao, H. Zhai, H. P. Zeng, W. Lu, G. J. Zhao, C. F. Yan, L. B. Su, and J. Xu, Appl. Phys. Lett. **89**, 101125 (2006).
[5]Y. H. Zong, G. J. Zhao, C. F. Yan, X. D. Xu, L. B. Su, and J. Xu, J. Cryst. Growth **294**, 416 (2006).
[6]F. Thibault, D. Pelenc, F. Druon, Y. Zaouter, M. Jacquemet, and P. Georges, Opt. Lett. **31**, 1555 (2006).
[7]S. Q. Man, E. Y. B. Pun, and P. S. Chung, Appl. Phys. Lett. **77**, 483 (2000).
[8]H. Lin, G. Meredith, S. B. Jiang, X. Peng, T. Luo, N. Peyghambarian, and E. Y. B. Pun, J. Appl. Phys. **93**, 186 (2003).
[9]R. S. Quimby, M. G. Drexhage, and M. J. Suscavage, Electron. Lett. **23**, 32 (1987).
[10]Y. H. Zong, G. J. Zhao, C. F. Yan, X. D. Xu, L. B. Su, and J. Xu, J. Cryst. Growth **294**, 416 (2006).
[11]S. F. Wong, E. Y. B. Pun, and P. S. Chung, IEEE Photonics Technol. Lett. **14**, 80 (2002).
[12]L. Zhang, H. F. Hu, and F. Y. Lin, Mater. Lett. **47**, 189 (2001).
[13]B. M. Walsh, N. P. Barnes, and B. di Bartolo, J. Appl. Phys. **83**, 2772 (1998).
[14]P. V. dos Santos, E. A. Gouveia, M. T. de Araujo, A. S. Gouveia-Neto, A. S. B. Sombra, and J. A. Medeiros Neto, Appl. Phys. Lett. **74**, 3607 (1999).